

Decay of counterflow He II turbulence in a finite channel: Possibility of missing links between classical and quantum turbulence

L. Skrbek, A. V. Gordeev, and F. Soukup

*Joint Low Temperature Laboratory, Institute of Physics ASCR and Charles University, V Holešovičkách 2,
180 00 Prague, Czech Republic*

(Received 21 January 2003; published 21 April 2003)

Decay of He II counterflow turbulence generated by applying a heat pulse to the closed end of a circular channel is investigated using second sound attenuation. Several orders of magnitude of decaying vortex line density display various regimes, starting with the inverse time decay predicted by Vinen towards distinct classical $t^{-3/2}$ power law occurring after saturation of the energy containing length scale by the size of the channel. The decaying counterflow turbulence displays a surprisingly close resemblance to recently reported decaying grid turbulence in He II, and both of them appear closely linked to classical grid generated turbulence.

DOI: 10.1103/PhysRevE.67.047302

PACS number(s): 47.27.Gs, 47.37.+q, 67.40.Pm, 67.40.Vs

Turbulence in superfluids [1] that are characterized by quantized circulation—quantum turbulence—along with classical turbulence in fluids described by the Navier-Stokes equations can be thought of as branches of a general physical phenomenon of fluid turbulence. There are similarities, but also important differences between the two, arising due to two-fluid behavior and quantization of circulation in superfluids.

Quantum turbulence is characterized by the existence of a tangle of quantized vortices [2]. Although recently an experimental detection of quantum turbulence in superfluid $^3\text{He-B}$ has been claimed [3], most attention has been paid to turbulent He II. Here the turbulence has recently been generated classically—in a flow past obstacles such as spheres [4] or grids [5–7] and in many cases closely resembles that in classical fluids [8]. This is particularly true for one of the cornerstone problems of turbulence—the decay of grid generated turbulence in a finite channel, which recently became better understood [9] when combining experimental data on decaying turbulent energy obtained in water with He II second sound attenuation data, spanning orders of magnitude of decaying vortex line density [6,7].

Although quantum turbulence in He II can be generated classically, historically it was discovered [10] in a counterflow channel, where it is easily generated by applying a heat pulse [2]. It has been emphasized many times (see, e.g., Ref. [11], and references therein) that counterflow turbulence has no classical analog and little attention was paid to possible links with classical turbulence. Indeed, in a limit of low flow velocities, He II displays extraordinary flow properties in close agreement with the phenomenological two-fluid model of Landau. The two-fluid model also predicts the existence of the second sound, serving as a very powerful tool in experimental investigation of quantum turbulence above ≈ 1 K.

Experimentally, counterflow turbulence has a long history since the discovery of superfluidity, beginning with the heat transport experiments through capillaries and channels of various sizes (e.g., Ref. [12], for a review, see Ref. [2]).

The counterflow turbulence in a wide channel was first investigated in pioneering experiments by Vinen [10], who also introduced a phenomenological model for its description

based on the concept of a random vortex tangle of a line density L . His equation of a form

$$\frac{\partial L}{\partial t} = \frac{\rho_n B}{2\rho} \chi_1 v_{ns} L^{3/2} - \frac{\kappa}{2\pi} \chi_2 L^2, \quad (1)$$

where $B = B(T)$ [13] is the mutual friction coefficient, v_{ns} is the counterflow velocity of the two fluids, ρ and ρ_n are the total and normal fluid densities, κ is the circulation quantum, and χ_1, χ_2 are phenomenological constants, was later deduced by Schwarz [14] using rather general arguments tracing back to the equation of vortex motion in the local approximation. Under the assumption that the vortex tangle is homogeneous, this approach accounts for most of the observed phenomena in steady state counterflow turbulence. It can also be applied to the transient response of the vortex tangle from one steady state towards another, and even allows an analytical solution [15], which for a particular case of free decay reduces to the inverse time dependence $L(t) \propto 1/(t + t_{vo})$, where t_{vo} stands for the virtual origin time [9].

The transient behavior of superfluid turbulence, and the free decay of the counterflow turbulence in particular, was experimentally investigated by many authors, e.g., Refs. [2,10,15–17]. The most peculiar feature of the experiment is an anomalously slow decay of $L(t)$ after switching off the heat input when v_{ns} is suddenly reduced to zero. The approach in virtue of Vinen's equation, with the same scaling coefficients describing both the grow and decay of the vortex tangle, does not provide a full physical picture of decaying counterflow turbulence. So far the most sophisticated attempt to understand the underlying physics of this puzzle was due to Schwarz and Rozen [15,17], who tackled the problem both experimentally and theoretically, and argued that “this regime should be interpreted in terms of a coupled turbulence in which random superfluid and normal motion interact with the vortex tangle, the whole system decaying self-consistently at a rate controlled by the normal fluid viscosity.” Indeed, their experimental data qualitatively agree with calculated decay curves of suggested phenomenological model based on homogeneous tangle that involves coupling

term between the two fluids and the newly introduced decay term via normal fluid viscosity.

In view of recent results indicating close resemblance of the grid generated He II turbulence with classical turbulence in Navier-Stokes fluids [7,9], we have applied the powerful experimental technique of second sound attenuation to experimentally investigate the decay of counterflow turbulence in a circular channel ($D=9$ mm in diameter, 13 cm long). The decaying vortex line density is deduced from the time dependent amplitude $A(t)$ of the standing wave of second sound, generated and detected by two identical plane gold-plated membranes acting as transducer and receiver, placed opposite each other across a channel in the middle of its length, so that the cross section of the main flow channel stays clear. The cylindrical space between transducer and receiver acts as a second sound resonator. Our detection technique is similar to that described in Refs. [5–7], but in order to eliminate the influence of connecting leads we developed an ultralow noise broadband current preamplifier and included it into our detection channel between the receiver membrane and the lock-in amplifier clocked by the fundamental resonance frequency of the second sound standing wave across the channel. The closed end of the channel includes a manganin wire heater wound on a conical surface. The channel is open to the He II bath and covered by another cone, in order to reduce coupling of the generated second sound signal with longitudinal modes in the channel along its length. The continuously applied heat input is switched between the channel heater and another matching one placed outside the channel in the He II bath in order to keep the applied power constant to assure best temperature control, finally tuned by the temperature controller via an additional bath heater.

The typical family of decay curves measured at 1.6 K is shown in Fig. 1. In order to compare the decay data with the classical turbulence data, we display the results in terms of vorticity ω assuming that, on average, $\omega \cong \kappa L$ in the same virtue as it was done in Refs. [7,9]. The decaying vortex line density includes the amplitude ratio $A_0/A(t)$ of second sound standing waves across the channel resonator, measured at fundamental frequency typically around 900 Hz, where A_0 stands for that without applied power into the channel [18]:

$$\omega(t) = \frac{8u_2}{\pi BD} \ln \frac{1 + \left(\frac{A_0}{A}\right)^2 a + \sqrt{2\left(\frac{A_0}{A}\right)^2 a + \left(\frac{A_0}{A}\right)^4 a^2}}{1 + a + \sqrt{2a + a^2}}, \quad (2)$$

where $a = 1 - \cos(2\pi D\Delta_0/u_2)$, Δ_0 is the full width at half height of the second sound resonance peak (typically 10 Hz) and u_2 stands for the second sound velocity. For our geometry and ω up to about 10^3 Hz (when $a \leq 10^{-7}$) Eq. (2) is well approximated by a simpler relation [10]

$$\omega(t) \cong \frac{16\Delta_0}{B} \left(\frac{A_0}{A} - 1 \right). \quad (3)$$

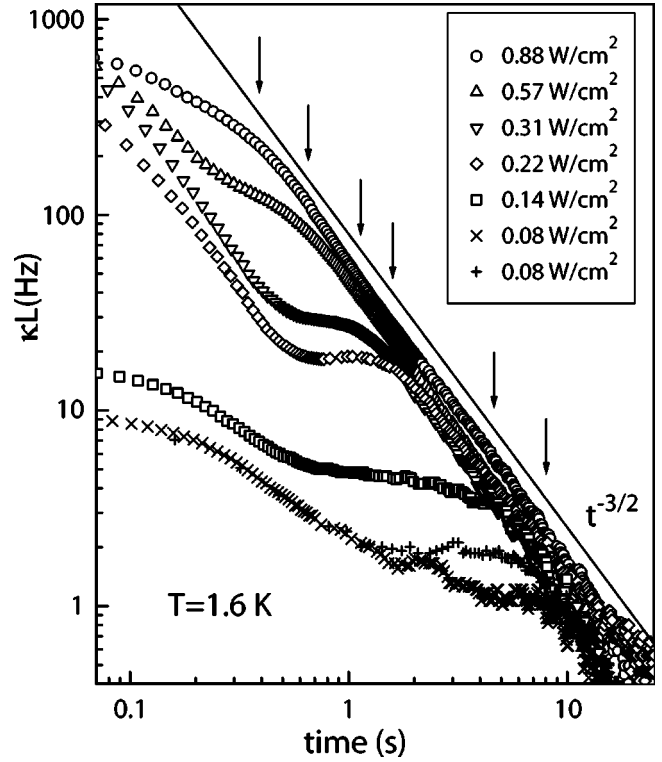


FIG. 1. The decay of vortex line density in counterflow turbulence measured at 1.6 K for various initial heat inputs as indicated. The saturation times t_{sat} after which the decay displays classical character of the form $t^{-3/2}$ are marked by arrows. Reproducibility of the data becomes an issue for decay curves originating from low starting values of L .

Our main observation and the most striking feature of all the data at $1.3 \text{ K} \leq T \leq 1.8 \text{ K}$ is that the late stage of the decay of counterflow turbulence displays several orders of magnitude of the classical $t^{-3/2}$ power law [19]. This law is obeyed after the saturation time, marked for each decay curve in Fig. 1 by a vertical arrow. For $t < t_{sat}$, the decay displays complicated features; sometimes even includes periods with slight net grow of L . However, as shown in Fig. 2, the early stage of decay of very high vortex line density displays the Vinen's decay of the form $(\kappa L)^{-1} \propto (t + t_{vo})$, which directly switches into a classical decay regime $(\kappa L)^{-2/3} \propto t$.

Similarly as in the case of the decay of He II turbulence generated by a towed grid, the character of the decay of counterflow turbulence hardly changes with temperature, despite a considerable change of the superfluid to the normal fluid density ratio. This strongly suggests that for $t > t_{sat}$ the decaying counterflow and grid generated He II turbulence are similar in character, especially while taking into account the ‘‘Reynolds number’’ dependence of the saturation time t_{sat} defined experimentally as a time when the decay switches into the classical $t^{-3/2}$ power law decay (see Fig. 1). Here we define the counterflow He II Reynolds number as $\text{Re}_{\text{He II}}^{\text{CF}} = Dv_{ns}\rho/\eta$, where the kinematic viscosity of He II is based on the dynamic viscosity of the normal fluid and the total density, i.e., $\nu = \eta/(\rho_n + \rho_s)$. Figure 3 displays the experimentally determined t_{sat} versus $\text{Re}_{\text{He II}}^{\text{CF}}$ at three different tem-

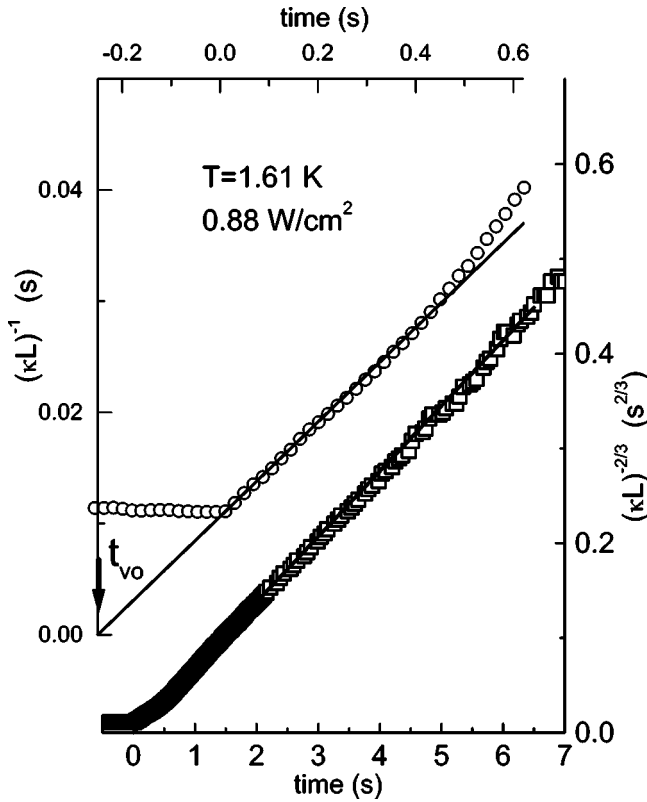


FIG. 2. The early stage of decay of vortex line density in counterflow turbulence measured after switching off the high rate of heating into the channel. The Vinen decay $(\kappa L)^{-1} = C_0(t + t_{vo})$ with $C_0 = 0.0425$ and virtual origin time (see arrow) $t_{vo} = 0.25$ s switches directly into a classical decay regime $(\kappa L)^{-2/3} = C_1 t$ with $C_1 = 0.69 \text{ s}^{1/3}$.

peratures. On the first approximation $t_{sat}(T) = t_{sat} \propto 1/\text{Re}_{\text{He II}}^{CF}$, thus behaving in close analogy with the data obtained in grid generated turbulence [7]. The agreement is especially good for the decay data starting from very high

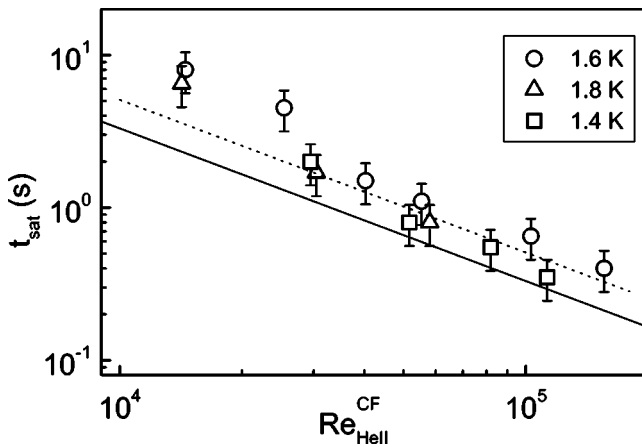


FIG. 3. The $\text{Re}_{\text{He II}}^{CF}$ dependence of the saturation times, measured at various temperatures as indicated. The solid line represents $\gamma/\text{Re}_{\text{He II}}^{CF}$ with $\gamma = 3.3 \times 10^4$, adopted from Ref. [7]. The broken line, corresponding to $\gamma_{corr} = 1.54\gamma$, accounts for the Re_M definition in towed grid turbulence [20].

line density in the channel, best representing the fully developed turbulence. Quantitative comparison of magnitudes of t_{sat} in grid generated and counterflow turbulence is not straightforward, due to the definition of the $\text{Re}_{\text{He II}}^{CF}$ [20] as well as slightly different channel size [21] and geometry. There is a call for further experiments allowing investigation of the decay of grid and counterflow turbulence in the same channel and with well defined grid geometry, but our view is that the striking similarity between decaying counterflow and grid turbulence in He II has been firmly established.

It is natural to ask whether any kind of a similarity between counterflow and grid generated He II turbulence is in some form built in already in a steady state counterflow turbulence. Any approach based on the assumption of homogeneous vortex tangle in steady state, such as Refs. [10,15], automatically rules out such a similarity and leaves the only explanation that this similarity builds up during the decay, after the driving force, i.e., the applied heat had been switched off. The homogeneous tangle approach is supported by experiments in Ref. [22], where no appreciable difference of the tangle properties has been found across the channel cross section [23]. However, in view of presented results, we speculate that this scenario seems unlikely. Although the concept of homogeneous tangle is a good approximation and explains steady state counterflow turbulence fairly well, we believe that the counterflow tangle is slightly polarized and organized in such a way that it “knows” about the size of the channel via suitably defined Reynolds number such as $\text{Re}_{\text{He II}}^{CF}$.

First of all, at all temperatures the measured saturation time scales roughly inversely proportionally with $\text{Re}_{\text{He II}}^{CF}$, in agreement with the quasiclassical behavior of this quantity in grid generated turbulence [7]. Still, one can argue that this scaling occurs due to viscous action of the normal fluid during the decay, after the channel heater had been switched off. However, the experimental fact that for constant initial $\text{Re}_{\text{He II}}^{CF}$ within the experimental accuracy $t_{sat}(T) \cong t_{sat}$ and thus does not appreciably depend on ρ_s/ρ_n (both in the decay of counterflow and grid generated He II turbulence) strongly suggests that the Reynolds number information is already inherently built in when the decay starts. We find it hard to believe that considerably different amount of normal fluid changes over the expected $1/t$ behavior that follows from the homogeneous tangle approach into classical $1/t^{3/2}$ power law within the same t_{sat} time.

In order to further support our point of view, let us consider the counterflow turbulence from standpoint of experimental facts known for the heat transfer efficiency in He II. At low heat loads, the heat transport between two He II reservoirs of different temperatures connected with the channel has no classical analogy, but we argue here, that at high heat loads the system closely resembles the heat transfer occurring in turbulent thermal convection in classical fluid between ideally thermally conducting bottom and top plates in a gravitational field. The efficiency of the heat transfer is given here by the Nusselt number Nu that compares how many times more effective turbulent convection is in comparison with molecular conduction only. The dynamical parameter is the dimensionless Rayleigh number Ra that re-

flects the fluid properties, the temperature difference ΔT between the plates, and the size of the whole system. It is of fundamental interest to know how Nu scales with $Ra \propto \Delta T$. Although the exact scaling $Nu \propto Ra^\beta$ remains an open question, most experiments in turbulent thermal convection suggest $\beta \cong 2/7$ that gradually increases towards $\beta \cong 1/3$. We have revisited and scanned experimental data of Chase [12] who carefully measured the heat transport by thermal counterflow in turbulent He II through connecting circular channels and found that these data once again display strong similarity with classical behavior, i.e., that in wide temperature range the overall heat transfer rate scales as $\dot{Q} \propto (\Delta T)^\beta$ with exponent β close to $2/7$ later rising to about $1/3$ with increasing ΔT in strikingly similar manner with classical turbulent thermal convection. Due to different geometry (high aspect ratio), more quantitative comparison is perhaps not possible. One can imagine, however, that the two He II reservoirs, thanks to extremely high thermal conductivity of He II, play a role of the ideally conducting bottom and top plates, while the chemical potential of He II replaces the gravitational potential in classical convection. Let us point out that within the two-fluid model the superfluid does not carry any heat, so the entire heat transfer occurs via the vis-

cous normal fluid. The presence of the vortex tangle in superfluid results in mutual friction and additional dissipation channel, but it seems this could be, at least approximately, taken into account by introducing an effective kinematic viscosity in analogy with the grid turbulence in He II [8,24]. There is a clear call for carefully designed experiments enabling more rigorous comparison of turbulent thermal convection with the heat transfer by the counterflow He II turbulence.

In conclusion, we have investigated the decay of counterflow He II turbulence in a finite size circular channel and found features strikingly similar to the decay of classical and grid generated He II turbulence. We believe that further investigation of links between superfluid (both counterflow and classically generated) and classical turbulence ought to bring more information on the fascinating field of fluid turbulence in general.

The authors acknowledge help and fruitful discussions with R. J. Donnelly, Z. Janu, M. Krusius, J. J. Niemela, M. Rotter, J. Šebek, K. R. Sreenivasan, M. Tsubota, and W. F. Vinen. The support of the Czech Grant Agency by the Grant No. GAČR 202/02/0251 is greatly appreciated.

-
- [1] *Quantized Vortex Dynamics and Superfluid Turbulence*, edited by C.F. Barenghi, R.J. Donnelly, and W.F. Vinen (Springer, New York, 2001).
- [2] J.T. Tough, *Superfluid Turbulence*, Progress in Low Temperature Physics Vol. VIII (North-Holland, Amsterdam, 1982).
- [3] S.N. Fisher *et al.*, Phys. Rev. Lett. **86**, 244 (2001).
- [4] M. Niemetz, H. Kerscher, and W. Schoepe, J. Low Temp. Phys. **126**, 287 (2002).
- [5] M.R. Smith *et al.*, Phys. Rev. Lett. **71**, 2583 (1993).
- [6] S.R. Stalp, L. Skrbek, and R.J. Donnelly, Phys. Rev. Lett. **82**, 4831 (1999).
- [7] L. Skrbek, J.J. Niemela, and R.J. Donnelly, Phys. Rev. Lett. **85**, 2973 (2000).
- [8] W.F. Vinen, Phys. Rev. B **61**, 1410 (2000).
- [9] L. Skrbek and S.R. Stalp, Phys. Fluids **12**, 1997 (2000).
- [10] H.E. Hall and W.F. Vinen, Proc. R. Soc. London, Ser. A **238**, 204 (1956); **238**, 205 (1956); W.F. Vinen, *ibid.* **240**, 114 (1957); **240**, 128 (1957); **242**, 489 (1957).
- [11] W.F. Vinen and J.J. Niemela, J. Low Temp. Phys. **128**, 167 (2002).
- [12] C.E. Chase, Phys. Rev. **127**, 361 (1962); **131**, 1898 (1963).
- [13] R.J. Donnelly and C.F. Barenghi, J. Phys. Chem. Ref. Data **27**, 1217 (1998).
- [14] K.W. Schwarz, Phys. Rev. B **38**, 2398 (1988).
- [15] K.W. Schwarz and J.R. Rozen, Phys. Rev. B **44**, 7563 (1991).
- [16] F.P. Milliken, K.W. Schwarz, and C.W. Smith, Phys. Rev. Lett. **48**, 1204 (1982).
- [17] K.W. Schwarz and J.R. Rozen, Phys. Rev. Lett. **66**, 1898 (1991).
- [18] S.R. Stalp, Ph.D. thesis, University of Oregon, Eugene, 2000 (unpublished).
- [19] Similar behavior was observed in rectangular counterflow channel 1×1 cm² (see Fig. 2 of Ref. [5]), but was not discussed or systematically investigated.
- [20] For the grid turbulence, the definition of the mesh Reynolds number $Re_M = \rho V_g M / \eta$ was used, where M is the mesh size and V_g is the velocity of the towed grid. For comparison with the counterflow the towing velocity ought to be enhanced, due to finite transparency of the monoplane 65% open grid [5], as the fluid passes through each opening of the grid on the average with the velocity exceeding that of towed grid by a factor of 1.54.
- [21] In contrast to our circular channel 9 mm in diameter, the grid turbulence channel was of square 1×1 cm² cross section. According to scaling arguments of homogeneous approach of Schwarz [14] one expects a scaling factor of order unity, 0.9^2 , while comparing the saturation times.
- [22] D.D. Awschalom, F.P. Milliken, and K.W. Schwarz, Phys. Rev. Lett. **53**, 1372 (1984).
- [23] The used ion technique, however, cannot be used close to the channel wall [22], where v_n cannot be constant in view of a nonslip boundary condition for the normal fluid. Note also that our starting values of L by more than an order of magnitude exceed those of Ref. [22]. Issues such as turbulent states I and II [2] or turbulence in the normal fluid might be relevant here.
- [24] See, e.g., *Quantized Vortex Dynamics and Superfluid Turbulence* (Ref. [1]), p. 85.